

Nuclear pasta and supernova neutrinos at late times

C. J. Horowitz,^{1,*} D. K. Berry,¹ M. E. Caplan,¹ T. Fischer,²
Zidu Lin,¹ W. G. Newton,³ E. O'Connor,⁴ and L. F. Roberts⁵

¹*Center for Exploration of Energy and Matter and Department of Physics,
Indiana University, Bloomington, IN 47405, USA*

²*Institute for Theoretical Physics, University of Wrocław, plac Maksa Borna 9, 50-204 Wrocław, Poland*

³*Department of Physics and Astronomy, Texas A&M University-Commerce, Commerce, TX 75429, USA*

⁴*Department of Physics, North Carolina State University, Raleigh, NC 27695, USA; Hubble Fellow*

⁵*National Superconducting Cyclotron Laboratory and Department of Physics and Astronomy,
Michigan State University, East Lansing, Michigan 48824, USA*

(Dated: February 15, 2022)

Nuclear pasta, with nucleons arranged into tubes, sheets, or other complex shapes, is expected in core collapse supernovae (SNe) at just below nuclear density. We calculate the additional opacity from neutrino-pasta coherent scattering using molecular dynamics simulations. We approximately include this opacity in simulations of SNe. We find that pasta slows neutrino diffusion and greatly increases the neutrino signal at late times of 10 or more seconds after stellar core collapse. This signal, for a galactic SN, should be clearly visible in large detectors such as Super-Kamiokande.

PACS numbers:

About 20 neutrinos were detected from supernova SN 1987A [1] confirming the radiation of $\approx 3 \times 10^{53}$ ergs of gravitational binding energy gained during the stellar core collapse. Several thousands of events are expected from the next galactic core collapse supernova (SN) [2]. These neutrinos carry information about the incompletely known explosion mechanism [3–5] and on nucleosynthesis in material ejected from the newly formed neutron star (or proto-neutron star PNS) by the intense neutrino flux [6–12]. SN neutrinos may undergo rich, possibly nonlinear, flavor oscillations [13, 14]. Finally the neutrino signal, in concert with gravitational-wave [15] and electromagnetic observations, may provide a historic multi-messenger data set.

During the SN explosion, the PNS deleptonizes and cools via the emission of neutrinos of all flavors. The associated neutrino signal at late times may be sensitive to PNS convection [16], neutrino interactions at high densities [17, 18], and the possibility of matter falling back onto the PNS. Finally, the neutrino signal will be dramatically modified if the star collapses to a black hole. New neutrino detectors [2] such as the Deep Underground Neutrino Experiment (DUNE) [19, 20] and Hyper-Kamiokande [21, 22] offer exciting capabilities. DUNE should provide detailed information on electron neutrinos while Hyper-K, with its very large volume, should be particularly good at observing SN neutrinos at late times.

In the PNS interior, densities in excess of nuclear saturation density $\approx 3 \times 10^{14}$ g/cm³ are reached. At just below nuclear density, nuclei are expected to rearrange into nuclear pasta structures with complex tube (spaghetti), sheet (lasagne), or other shapes [23]. These shapes arise because of the competition between short-range nuclear attraction and long-range Coulomb repulsion. SN neu-

trinos, with 10s of MeV energies, have wavelengths comparable to the size of these shapes and will scatter coherently from all of the nucleons inside [24, 25]. This scattering may increase the opacity and significantly impact the neutrino signal from core collapse SN.

Recently there have been several calculations of nuclear pasta structure, see for example [26–34]. There are interesting similarities between spiral shapes that might be present in both nuclear pasta and biological membranes, despite the two systems differing in density by 14 orders of magnitude [35], see also [36]. Observational signatures of pasta in older neutron stars have recently been discussed: if disordered, pasta could cause magnetic field decay [37] and slow the cooling of neutron star crusts [38, 39].

In this letter we demonstrate a new observational signature of pasta in PNSs. We calculate neutrino-pasta scattering cross sections by performing large-scale molecular dynamics simulations of nuclear pasta. We approximately include these cross sections in astrophysical simulations of core-collapse and PNS cooling. For the first time, we predict the impact of pasta on neutrino luminosities and mean energies. Finally, we predict the signal, from a galactic SN in a large water detector such as Super-Kamiokande [40]. We find that the signal could be significantly enhanced at late times of 10 or more seconds after stellar core collapse, as nuclear pasta tends to slow neutrino diffusion.

Neutrino-nucleon elastic scattering is modified in the medium by correlations and structure formation. We write the transport cross section per nucleon in the medium σ as $\sigma = \sigma_0 S_{\text{tot}}$ with σ_0 the free transport cross section. The total response S_{tot} describes the medium modifications. It depends on the vector response S_V , that describes the response of the system to vector currents,

and the axial response S_A , that describes the response to axial (or spin) currents, see for example Eq. 31 of Ref. [41],

$$S_{\text{tot}} = (1 + \xi f_{\text{pasta}}) = \frac{(1 - Y_p)S_V + 5g_a^2 S_A}{1 - Y_p + 5g_a^2}. \quad (1)$$

Here $g_a = -1.26$ and the proton fraction is Y_p . For later use, we have also defined ξf_{pasta} as the enhancement in S_{tot} , from pasta, over the free response $S_V = S_A = 1$. Here ξ is a constant encoding the maximum enhancement and $0 \leq f_{\text{pasta}}(n_b, T, Y_p) \leq 1$ encodes the density n_b , temperature T , and proton fraction Y_p region over which pasta is present.

The vector response S_V is an appropriate integral of the neutron static structure factor $S_n(q)$ over momentum transfer q [24],

$$S_V(E_\nu) = \frac{3}{4} \int_{-1}^1 d\cos\theta (1 - \cos^2\theta) S_n(q). \quad (2)$$

Here q depends on the neutrino energy E_ν and scattering angle θ , $q^2 = 2E_\nu^2(1 - \cos\theta)$. For complex nuclear pasta phases, we calculate $S_n(q)$ using (semi)classical molecular dynamics (MD) simulations,

$$S_n(q) = \langle \rho(q)^* \rho(q) \rangle. \quad (3)$$

Here the neutron density in momentum space is $\rho(q) = N^{-1/2} \sum_{i=1}^N \exp[i\mathbf{q} \cdot \mathbf{r}_i]$ with $\mathbf{r}_i(t)$ the location of the i th neutron, N the total number of neutrons in the simulation, and the average in Eq. 3 is taken over simulation time t . Sample configurations from our MD simulations are shown in Fig. 1. We use the model in ref. [24]. Sonoda et al. [42] have also calculated $S_V(E_\nu)$ in a slightly different QMD model, although for smaller systems with possibly larger finite size effects. They find qualitatively similar results.

Figure 2 shows $S_V(E_\nu)$, Eq. 2, calculated from our MD simulations. Our MD model has been used to study nuclear pasta in many previous works [24, 25, 27, 35, 43–46]. An initial random configuration, at a density $n = 0.12 \text{ fm}^{-3}$, is evolved to the desired density by slowly expanding the simulation volume at a rate of 10^{-8} c/fm . Next the system is equilibrated for at least $9 \times 10^7 \text{ fm/c}$ at constant density, using an MD time step of 2 fm/c . Then $S_n(q)$ is calculated as a time average of at least 180,000 configurations, each separated by $1,000 \text{ fm/c}$. This involves an additional time evolution of at least $1.8 \times 10^8 \text{ fm/c}$. An advantage of this molecular dynamics simulation is that $S_n(q)$ can be directly determined. Unfortunately this model is likely most accurate at low temperatures and high proton fractions. Therefore, the above simulations were done at a temperature of $T = 1 \text{ MeV}$ and a proton fraction $Y_p = 0.4$. We expect results for other temperatures and proton fractions to be qualitatively similar as long as the basic sizes of the pasta pieces are similar.

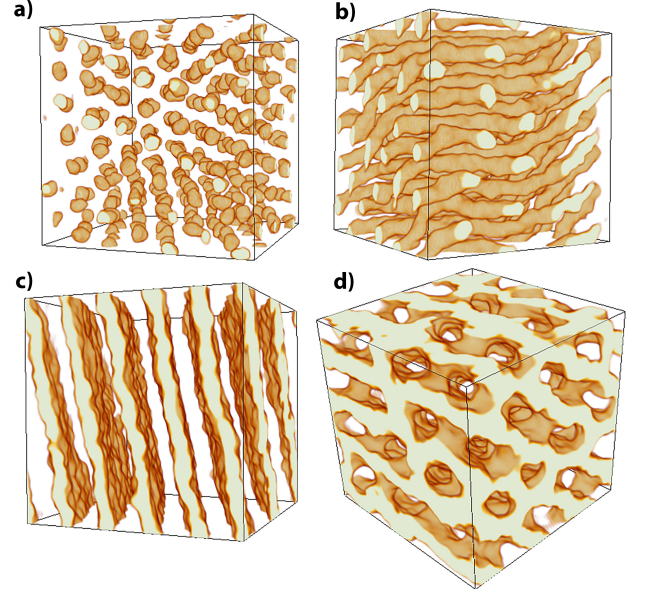


FIG. 1: (color on line) Sample configurations from MD simulations with 51,200 nucleons, that show the following shapes, at densities of a) 0.01 (isolated nuclei), b) 0.025 (tubes), c) 0.05 (sheets), and d) 0.075 fm^{-3} (cylindrical holes).

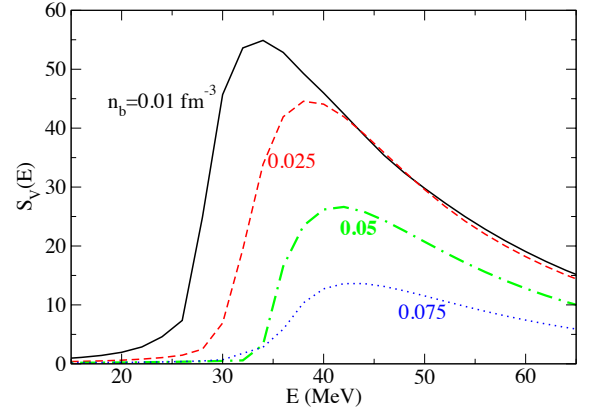


FIG. 2: (color on line) Molecular dynamics simulation results for the static structure factor $S_V(E)$ averaged over scattering angles, see Eq. 2, vs neutrino energy E . Curves are based on simulations with 51200 nucleons and are at densities of 0.01 (solid), 0.025 (dashed), 0.05 (dot dashed) and 0.075 fm^{-3} (dotted).

We see that $S_V(E_\nu)$ in Fig. 2 can be as large as ≈ 50 . In contrast, the axial response S_A is not expected to be enhanced as the nucleon spins do not add coherently, see for example [41]. We are not aware of any explicit calculations of S_A for pasta and use $S_A \approx 1$ as a simple estimate. This leads to an enhancement for ξ , Eq. 1, that could be as large as $\xi \approx 5$.

Alternatively, we consider equations of state that include “spherical pasta” phases. Here, neutrino pasta scattering is modeled as neutrino nucleus elastic scattering from exotic neutron rich heavy nuclei that are assumed nearly spherical in shape but have strong Coulomb correlations between nuclei such that the effective static structure factor is [25],

$$S_n(q) \approx N S_{\text{ion}}(q) F(q)^2. \quad (4)$$

Here N is the neutron number of the heavy nucleus, $F(q)$ is the nuclear elastic form factor and $S_{\text{ion}}(q)$ is the static structure factor for charged ions [47]. This describes the correlations between nuclei at long wavelengths. These exotic heavy nuclei are expected to be present for PNS cooling conditions ≈ 3 or more seconds after stellar core collapse, see below. For the HS(DD2) equation of state [48], and using H. Shen’s nuclear composition [49], we find that neutrino scattering from these exotic heavy nuclei, calculated as in ref. [50], can increase the neutral current scattering opacity by up to a factor of $\xi \approx 5$ to 10. This enhancement is consistent with our estimate from MD simulations.

To determine the range of densities n_b and temperatures T where pasta may be present, we have performed fully quantum calculations using the NRAPR Skyrme functional [51]. These calculations are described in Ref. [52, 53]. At $Y_p = 0.3$, we find pasta phases for $n_b = 0.03$ to 0.11 fm^{-3} and up to a maximum $T = 11 \text{ MeV}$. This region slightly decreases with decreasing Y_p . For $Y_p = 0.1$, pasta is present for $n_b = 0.04$ to 0.09 fm^{-3} and up to $T = 7 \text{ MeV}$. At lower densities, large spherical nuclei will likely be present that will also increase the scattering. Therefore, the region with an enhanced neutrino opacity (compared to free nucleons) probably extends to somewhat lower densities. This is shown in Fig. 1 a) and Fig. 2 where the $n_b = 0.01 \text{ fm}^{-3}$ MD simulation actually involves nucleons clustered into isolated nuclei.

We explore two phases of core collapse SN where pasta may impact the thermodynamics and neutrino emission. Pasta is included parametrically by enhancing the neutrino scattering opacity in regions where we expect the pasta to be present. This region is defined by $f_{\text{pasta}} = h(n_b/n_{\text{min}} - 1, 0.3)h(1 - n_b/n_{\text{max}}, 0.1)h(1 - T/T_{\text{crit}}, 0.1)$, where $h(x, y) = 1/2 + 1/2 \tanh(x/y)$. The scattering opacity is then corrected to be $\kappa_s = \kappa_{s,0}(1 + \xi f_{\text{pasta}})$, where $\kappa_{s,0}$ is the scattering opacity in the absence of pasta. Based on the results of our pasta calculations, we choose $n_{\text{min}} = 0.01 \text{ fm}^{-3}$, $n_{\text{max}} = 0.1 \text{ fm}^{-3}$, and $T_{\text{crit}} = 10 \text{ MeV}$. We expect that changing these parameters will impact the details of how pasta impacts our simulations, but these suffice for exploratory calculations.

The first presence of pasta occurs late in the collapse phase, $\sim 1 \text{ ms}$ prior to core bounce (when nuclear density is reached). We explore this phase with one-dimensional collapse simulations using GR1D [54]. The pasta is located well inside the electron neutrino decoupling radius

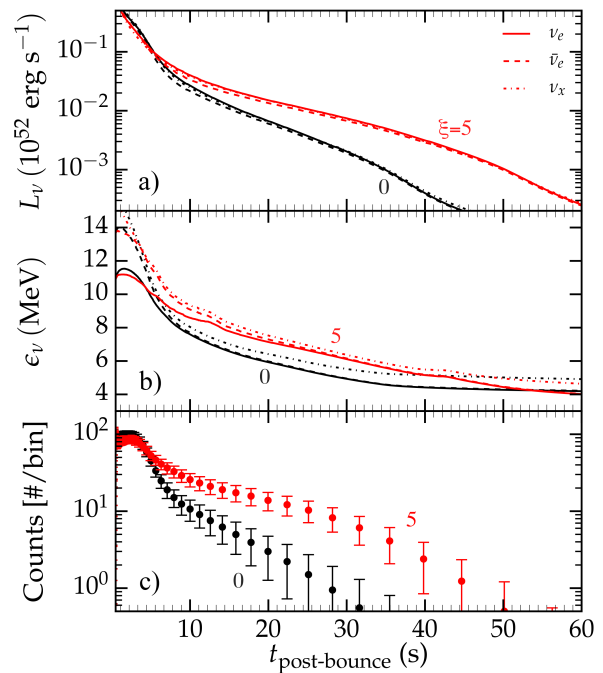


FIG. 3: (Color on line) Neutrino luminosity a) (top), mean neutrino energy b) (middle), and approximate number of Super-Kamiokande counts at 10 kpc c) (bottom) versus time since core bounce. Shown is the baseline simulation with no opacity enhancement ($\xi = 0$, black), and one simulation using $\xi = 5$ (red). The counts are shown for logarithmically spaced time bins and the error bars are Poissonian. The presence of pasta enhances the neutrino luminosity in all flavors at late times and also increases the average energies of all flavors of neutrinos. These two effects combine to significantly increase the count rate at late times for models including pasta.

and since these neutrinos make up the bulk of the neutrino energy density at this time, we see no dynamic or thermodynamic effect of the presence of pasta. However, there is a perceptible, yet very small impact on the ν_x signal at this time. The decoupling density for ν_x , for a very brief time, reaches upwards of $\sim 8 \times 10^{12} \text{ g cm}^{-3}$. With the presence of pasta, we see a suppression in the ν_x luminosities of $\sim 3 - 4$ times, in the millisecond preceding bounce. Since the ν_x luminosity at this point is only $\sim 10^{49} \text{ erg s}^{-1}$ and the average neutrino energy is low, we do not expect this effect to be observable with current or even next generation detectors.

Although the impact of pasta on the infall phase neutrino emission is very small, it may significantly alter the late time neutrino cooling signal when pasta forms in the atmosphere of the PNS. Using a variant of the spherically symmetric radiation hydrodynamics code described in [55], we evolve a $15 M_{\odot}$ progenitor [56] from core collapse through the accretion phase. Once the shock has passed a baryonic mass coordinate of $1.5 M_{\odot}$, we excise the outer layers of the star and evolve only the PNS over 100 s. Convection is included as in [16] through a mixing

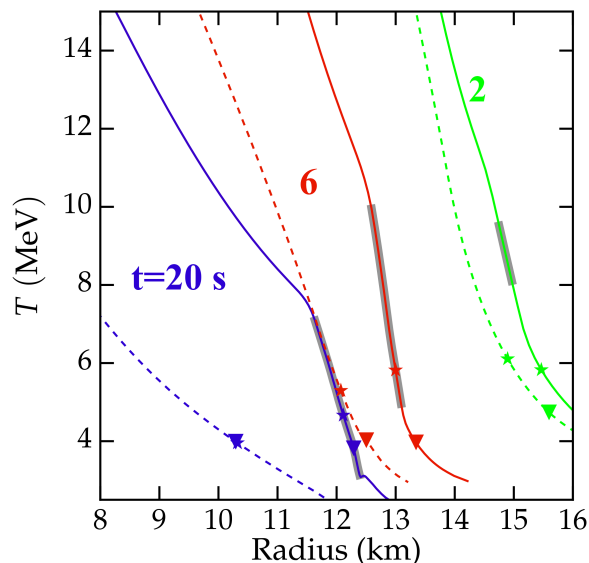


FIG. 4: (Color on line) Temperature structure of the PNS atmosphere versus radius with (solid lines, $\xi = 5$) and without (dashed lines, $\xi = 0$) parameterized pasta. The pasta is present in the gray regions. The green, red, and blue lines are for times $t = 2, 6$, and 20 s after core collapse, respectively. The triangles and stars correspond to the electron neutrino and anti-neutrino spheres, respectively. The critical temperature of the pasta prevents the inner layers of the atmosphere from reducing their temperature, resulting in a hotter, extended atmosphere. This results in the larger luminosities and neutrino average energies in models including pasta.

length theory prescription. We employ a new implementation of the LS220 EoS [57, 58] and we use the simple neutrino opacities of [59]. We expect more realistic opacities for homogeneous material to change the cooling timescale, but not qualitatively impact the difference between models with and without pasta [9, 16, 17].

Here we present two models, one without parameterized pasta opacities $\xi = 0$ and one with parameterized pasta opacities $\xi = 5$. In Fig. 3, the neutrino emission properties of these two models are shown. Pasta enhances the late time neutrino luminosity and the average energies of all neutrino species are increased. This is due to the impact of pasta on the PNS atmosphere, where pasta forms at late times. The temperature structure of the atmosphere at select times is shown in Fig. 4. The pasta is present at one second after bounce near the surface of the PNS and persists until late times. Rather than cooling to a low temperature, the interior of the PNS tries to stay above the pasta critical temperature to maintain a low opacity and increase the rate of energy transport. This results in a stronger temperature gradient near the PNS surface, a higher temperature of neutrino decoupling, and a more radially extended atmosphere. The higher decoupling temperature increases the neutrino average energies, while the larger radius and

increased decoupling temperature both serve to increase the neutrino luminosities. We expect the results to be sensitive to the critical temperature. If T_{crit} is smaller than we have assumed, we expect a smaller impact on the neutrino emission.

In the bottom panel of Fig. 3 we show the expected count rates for these models in Super-Kamiokande calculated using the SNOwGLOBES package [2]. We assume a distance of 10 kpc, a detector mass of 32 kT, and for simplicity only include inverse beta decay events from $\bar{\nu}_e$. The total number of events is about 3400. Clearly, the pasta has a strong impact on the late time detection prospects and can enhance the count rate by almost an order of magnitude. For the two particular models considered here, only 51 ± 7 counts are expected after 10 seconds for the model without pasta while 181 ± 13 counts are expected for the model including pasta. Both the enhanced luminosity and the larger average energies increase detection efficiency. Therefore, a signature of the nuclear pasta should be visible in the late-time neutrino signal of a galactic CCSN.

Future work should improve the calculation of neutrino-pasta scattering and how this, and its energy dependence, is incorporated into proto-neutron star cooling simulations. In addition, the late time neutrino signal should be studied in more detail for large detectors such as Super-K, Hyper-K, or possibly Ice Cube [60].

In conclusion, we have used molecular dynamics simulations to calculate neutrino-pasta scattering and approximately included this in simulations of proto-neutron star cooling. We find that nuclear pasta can slow the diffusion of neutrinos and significantly enhance the late time neutrino signal at times of 10 to 100 seconds after stellar core collapse. This signal, for a galactic SN, should be clearly visible in large neutrino detectors such as Super-Kamiokande, and its observation could provide information on neutrinos scattering from nuclear pasta shapes.

We thank Shirley Li and John Beacom for helpful discussions and the Institute for Nuclear Theory at the University of Washington where some of this work was done. This work was supported in part by DOE Grants DE-FG02-87ER40365 (Indiana University) and DE-SC0008808 (NUCLEI SciDAC Collaboration). Support for this work was provided also by NASA through Hubble Fellowship Grant #51344.001-A awarded by the Space Telescope Science Institute, which is operated by the Association of Universities for Research in Astronomy, Inc., for NASA, under contract NAS 5-26555. TF acknowledges support from the Polish National Science Center (NCN) under grant number UMO-2011/02/A/ST2/00306. WN was supported by the Research Corporation for Science Advancement through the Cottrell College Science Award #22741. This work was enabled in part by the NSF under Grant No. PHY-1430152 (JINA Center for the Evolution of the Elements). Computer time was provided by the INCITE

program. This research used resources of the Oak Ridge Leadership Computing Facility located at Oak Ridge National Laboratory, which is supported by the Office of Science of the Department of Energy under Contract No. DEAC05-00OR22725.

* Electronic address: horowit@indiana.edu

- [1] Maria Laura Costantini, Aldo Ianni, and Francesco Visani. Sn1987a and the properties of the neutrino burst. *Phys. Rev. D*, 70:043006, Aug 2004.
- [2] Kate Scholberg. Supernova neutrino detection. *Ann. Rev. Nuclear and Particle Science*, 62:81, 2012.
- [3] T. Lund, A. Marek, C. Lunardini, H.-T. Janka, and G. Raffelt. Fast time variations of supernova neutrino fluxes and their detectability. *Phys. Rev. D*, 82(6):063007, September 2010.
- [4] T. D. Brandt, A. Burrows, C. D. Ott, and E. Livne. Results from Core-collapse Simulations with Multi-dimensional, Multi-angle Neutrino Transport. *Astrophys. J.*, 728:8, February 2011.
- [5] I. Tamborra, F. Hanke, B. Müller, H.-T. Janka, and G. Raffelt. Neutrino Signature of Supernova Hydrodynamical Instabilities in Three Dimensions. *Phys. Rev. Lett.*, 111(12):121104, September 2013.
- [6] Y.-Z. Qian, G. M. Fuller, G. J. Mathews, R. W. Mayle, J. R. Wilson, and S. E. Woosley. Connection between flavor mixing of cosmologically significant neutrinos and heavy element nucleosynthesis in supernovae. *Phys. Rev. Lett.*, 71:1965–1968, September 1993.
- [7] C. J. Horowitz and Gang Li. Charge-conjugation violating neutrino interactions in supernovae. *Phys. Rev.*, D61:063002, 2000.
- [8] C. J. Horowitz. Supernova SN1987A bound on neutrino spectra for R-process nucleosynthesis. *Phys. Rev.*, D65:083005, 2002.
- [9] L. Hüpdepohl *et al.* Neutrino Signal of Electron-Capture Supernovae from Core Collapse to Cooling. *Phys. Rev. Lett.*, 104:251101, 2010.
- [10] T. Fischer *et al.* Protoneutron star evolution and the neutrino-driven wind in general relativistic neutrino radiation hydrodynamics simulations. *A&A*, 517:A80, 2010.
- [11] G. Martínez-Pinedo, T. Fischer, A. Lohs, and L. Huther. Charged-Current Weak Interaction Processes in Hot and Dense Matter and its Impact on the Spectra of Neutrinos Emitted from Protoneutron Star Cooling. *Phys. Rev. Lett.*, 109(25):251104, December 2012.
- [12] L. F. Roberts, S. Reddy, and G. Shen. Medium modification of the charged-current neutrino opacity and its implications. *Phys. Rev. C*, 86(6):065803, December 2012.
- [13] Huaiyu Duan, George M. Fuller, and Yong-Zhong Qian. Collective neutrino oscillations. *Annual Review of Nuclear and Particle Science*, 60:569, 2010.
- [14] M.-R. Wu, Y.-Z. Qian, G. Martínez-Pinedo, T. Fischer, and L. Huther. Effects of neutrino oscillations on nucleosynthesis and neutrino signals for an 18 M_{\odot} supernova model. *Phys. Rev. D*, 91(6):065016, March 2015.
- [15] S. E. Gossan, P. Sutton, A. Stuver, M. Zanolin, K. Gill, and C. D. Ott. Observing gravitational waves from core-collapse supernovae in the advanced detector era. *Phys. Rev. D*, 93:042002, Feb 2016.
- [16] L. F. Roberts, G. Shen, V. Cirigliano, J. A. Pons, S. Reddy, and S. E. Woosley. Protoneutron star cooling with convection: The effect of the symmetry energy. *Phys. Rev. Lett.*, 108:061103, Feb 2012.
- [17] S. Reddy, M. Prakash, J. M. Lattimer, and J. A. Pons. Effects of strong and electromagnetic correlations on neutrino interactions in dense matter. *Phys. Rev. C*, 59:2888–2918, May 1999.
- [18] Adam Burrows and R. F. Sawyer. Many-body corrections to charged-current neutrino absorption rates in nuclear matter. *Phys. Rev. C*, 59:510–514, Jan 1999.
- [19] Artur Ankowski *et al.* Supernova physics at dune. *arXiv:1608.07853*, 2016.
- [20] Maury Goodman. The Deep Underground Neutrino Experiment. *Adv. High Energy Phys.*, 2015:256351, 2015.
- [21] K. Abe *et al.* Physics potential of a long-baseline neutrino oscillation experiment using a j-parc neutrino beam and hyper-kamiokande. *Prog. Theor. Exp. Phys.*, 053C02, 2015.
- [22] Jost Migenda. *Detecting Fast Time Variations in the Supernova Neutrino Flux with Hyper-Kamiokande*. PhD thesis, Munich, Max Planck Inst., 2016.
- [23] D. G. Ravenhall, C. J. Pethick, and J. R. Wilson. Structure of matter below nuclear saturation density. *Phys. Rev. Lett.*, 50:2066–2069, Jun 1983.
- [24] Charles J. Horowitz, M. A. Perez-Garcia, and J. Piekarewicz. Neutrino-pasta scattering: The opacity of nonuniform neutron-rich matter. *Phys. Rev.*, C69:045804, 2004.
- [25] Charles J. Horowitz, M. A. Perez-Garcia, J. Carriere, D. K. Berry, and J. Piekarewicz. Nonuniform neutron-rich matter and coherent neutrino scattering. *Phys. Rev.*, C70:065806, 2004.
- [26] Bastian Schuetrumpf, Chunli Zhang, and Witold Nazarewicz. Clustering and pasta phases in nuclear density functional theory. *arXiv:1607.01372*, 2016.
- [27] A. S. Schneider, D. K. Berry, M. E. Caplan, C. J. Horowitz, and Z. Lin. Effect of topological defects on “nuclear pasta” observables. *Phys. Rev. C*, 93:065806, Jun 2016.
- [28] Rana Nandi and Stefan Schramm. Low-density nuclear matter with quantum molecular dynamics: The role of the symmetry energy. *Phys. Rev. C*, 94:025806, Aug 2016.
- [29] I. Sagert, G. I. Fann, F. J. Fattoyev, S. Postnikov, and C. J. Horowitz. Quantum simulations of nuclei and nuclear pasta with the multiresolution adaptive numerical environment for scientific simulations. *Phys. Rev. C*, 93:055801, May 2016.
- [30] B. Schuetrumpf and W. Nazarewicz. Twist-averaged boundary conditions for nuclear pasta hartree-fock calculations. *Phys. Rev. C*, 92:045806, Oct 2015.
- [31] U. J. Furtado, S. S. Avancini, J. R. Marinelli, W. Martarello, and C. Providencia. Neutrino diffusion in the pasta phase matter within the Thomas-Fermi approach. *Eur. Phys. J.*, A52(9):290, 2016.
- [32] B. Schuetrumpf, K. Iida, J. A. Maruhn, and P.-G. Reinhard. Nuclear “pasta matter” for different proton fractions. *Phys. Rev. C*, 90:055802, Nov 2014.
- [33] Toshiaki Maruyama, Gentaro Watanabe, and Satoshi Chiba. Molecular dynamics for dense matter. *Progress of Theoretical and Experimental Physics*, 01A201, 2012.
- [34] M. D. Alloy and D. P. Menezes. Nuclear “pasta phase” and its consequences on neutrino opacities. *Phys. Rev.*

- C*, 83:035803, Mar 2011.
- [35] D. K. Berry, M. E. Caplan, C. J. Horowitz, Greg Huber, and A. S. Schneider. “parking-garage” structures in nuclear astrophysics and cellular biophysics. *Phys. Rev. C*, 94:055801, Nov 2016.
 - [36] M. E. Caplan and C. J. Horowitz. Astromaterial Science and Nuclear Pasta. *arXiv:1606.03646*, 2016.
 - [37] Jose A. Pons, Daniele Vigano, and Nanda Rea. A highly resistive layer within the crust of x-ray pulsars limits their spin periods. *Nature Physics*, 9:431, 2013.
 - [38] C. J. Horowitz, D. K. Berry, C. M. Briggs, M. E. Caplan, A. Cumming, and A. S. Schneider. Disordered nuclear pasta, magnetic field decay, and crust cooling in neutron stars. *Phys. Rev. Lett.*, 114:031102, Jan 2015.
 - [39] Alex Deibel, Andrew Cumming, Edward F. Brown, and Sanjay Reddy. Late time cooling of neutron star transients and the physics of the inner crust. *arXiv:1609.07155*, 2016.
 - [40] Christopher W. Walter. The Super-Kamiokande Experiment. *arXiv:0802.1041*, 2008.
 - [41] C. J. Horowitz, O. L. Caballero, Zidu Lin, Evan O’Connor, and A. Schwenk. Neutrino-nucleon scattering in supernova matter from the virial expansion. *arXiv:1611.05140*, 2016.
 - [42] Hidetaka Sonoda, Gentaro Watanabe, Katsuhiko Sato, Tomoya Takiwaki, Kenji Yasuoka, and Toshikazu Ebisuzaki. Impact of nuclear “pasta” on neutrino transport in collapsing stellar cores. *Phys. Rev. C*, 75:042801, Apr 2007.
 - [43] C. J. Horowitz and D. K. Berry. The Shear Viscosity and Thermal Conductivity of Nuclear Pasta. *Phys. Rev.*, C78:035806, 2008.
 - [44] M. E. Caplan, A. S. Schneider, C. J. Horowitz, and D. K. Berry. Pasta nucleosynthesis: Molecular dynamics simulations of nuclear statistical equilibrium. *Phys. Rev. C*, 91:065802, Jun 2015.
 - [45] A. S. Schneider, D. K. Berry, C. M. Briggs, M. E. Caplan, and C. J. Horowitz. Nuclear “waffles”. *Phys. Rev. C*, 90:055805, Nov 2014.
 - [46] C. J. Horowitz, M. A. Perez-Garcia, D. K. Berry, and J. Piekarewicz. Dynamical response of the nuclear pasta in neutron star crusts. *Phys. Rev.*, C72:035801, 2005.
 - [47] C. J. Horowitz. Neutrino Trapping in a Supernova and Ion Screening. *Phys. Rev.*, D55:4577–4581, 1997.
 - [48] Matthias Hempel and Jrgen Schaffner-Bielich. A statistical model for a complete supernova equation of state. *Nuclear Physics A*, 837(3):210 – 254, 2010.
 - [49] H. Shen, H. Toki, K. Oyamatsu, and K. Sumiyoshi. Relativistic equation of state of nuclear matter for supernova and neutron star. *Nuclear Physics A*, 637:435–450, July 1998.
 - [50] A. Mezzacappa and S. W. Bruenn. Type II supernovae and Boltzmann neutrino transport - The infall phase. *Astrophys. J.*, 405:637–668, March 1993.
 - [51] A.W. Steiner, M. Prakash, J.M. Lattimer, and P.J. Ellis. Isospin asymmetry in nuclei and neutron stars. *Physics Reports*, 411(6):325 – 375, 2005.
 - [52] W. G. Newton and J. R. Stone. Modeling nuclear “pasta” and the transition to uniform nuclear matter with the 3d skyrme-hartree-fock method at finite temperature: Core-collapse supernovae. *Phys. Rev. C*, 79:055801, May 2009.
 - [53] Helena Pais, William G. Newton, and Jirina R. Stone. Phase transitions in core-collapse supernova matter at sub-saturation densities. *Phys. Rev. C*, 90:065802, Dec 2014.
 - [54] E. O’Connor. An Open-source Neutrino Radiation Hydrodynamics Code for Core-collapse Supernovae. *Astrophys. J. Supp.*, 219:24, August 2015.
 - [55] L. F. Roberts. A New Code for Proto-neutron Star Evolution. *Astrophys. J.*, 755:126, August 2012.
 - [56] S. E. Woosley, A. Heger, and T. A. Weaver. The evolution and explosion of massive stars. *Reviews of Modern Physics*, 74:1015–1071, November 2002.
 - [57] J. M. Lattimer and F. Swesty. A generalized equation of state for hot, dense matter. *Nuclear Physics A*, 535:331–376, December 1991.
 - [58] A. Schneider, L. F. Roberts, and C. D. Ott. A New Open-Source Nuclear Equation of State Framework based on the Liquid-Drop Model with Skyrme Interactions. *to be submitted to Phys. Rev. C.*, 2016.
 - [59] S. W. Bruenn. Stellar core collapse - Numerical model and infall epoch. *ApJS*, 58:771–841, August 1985.
 - [60] L. Köpke and IceCube Collaboration. Supernova Neutrino Detection with IceCube. *Journal of Physics Conference Series*, 309(1):012029, August 2011.